# A DFT study of the structures of pyruvic acid isomers and their decarboxylation

**Rita Kakkar,* Mallika Pathak and N. P. Radhika**

***Received 17th November 2005, Accepted 4th January 2006***
***First published as an Advance Article on the web 23rd January 2006***
**DOI: 10.1039/b516355b**

Pyruvic acid and its isomers, including the enol tautomers and enantiomeric lactone structures, have been investigated at the B3LYP/6-311 + + G(3df,3pd) level, and it is found that a keto form with *trans* $C_{methyl}C_{keto}C_{acid}O_{hydroxyl}$ and *cis* $C_{keto}C_{acid}OH$, and with one methyl hydrogen in a synperiplanar position with respect to the keto oxygen, is the most stable. This agrees with previous theoretical and experimental determinations. However, no minimum corresponding to protonated pyruvate could be located, although previous semiempirical calculations had found such structures. Decarboxylation by different possible routes was then studied. It was found that the direct formation of acetaldehyde, the most stable of the resulting $C_2H_4O$ isomers, *via* a four-center-like transition state is the most feasible, although there is a high activation barrier of 70 kcal $mol^{-1}$. In contrast to semiempirical calculations, it is found that no hydroxyethylidene–carbon dioxide complex exists as a product, and no transition state leading to the dissociation to hydroxethylidene could be located.

## Introduction

Pyruvic acid, $CH_3COCOOH$, is the traditional name for 2-oxopropanoic acid, a colorless liquid. Also known as pyroracemic acid, it is an organic acid first obtained by Berzelius by the dry distillation of tartaric or racemic acids.[1] It plays a fundamental role in biological systems, and occurs naturally in the body. It is an intermediate in the metabolism of carbohydrates, formed by the anaerobic glycolysis of glucose. It is then oxidized to carbon dioxide and acetic acid molecules, bonded to coenzyme A, or CoA. Alternatively, in the absence of sufficient oxygen, pyruvic acid may be reduced to lactic acid, responsible for muscle fatigue. Its anion, pyruvate ($CH_3COCOO^-$), is also an important intermediate compound in the carbohydrate metabolism of living organisms, and is the product of glycolysis and a precursor for the Krebs cycle.

Several kinetic studies on the decomposition of pyruvic acid have been reported in the literature. The decarboxylation reaction has been studied experimentally by both thermal and photodissociation methods.[2–5] There has also been considerable experimental interest in the relative magnitudes of the barriers to intramolecular rearrangements connecting acetaldehyde, vinyl alcohol and hydroxyethylidene, but agreement as to the ordering of the barriers has yet to be reached. There have been a number of *ab initio* studies of various aspects of the potential energy surface connecting the three isomers.[6–17]

We have therefore carried out a theoretical investigation of the pyruvic acid molecule and its isomers and some of their reactions. The preferred conformations of the pyruvic acid molecule, as well as its enol tautomer, were first determined. The vibrational spectra of the conformers were compared with the experimental spectra to confirm the most stable isomers. We then studied the decarboxylation pathways by three channels, leading, respectively, to acetaldehyde, hydroxyethylidene and vinyl alcohol. The interconversion of these three molecules was then investigated.

The pyruvic acid molecule is interesting from the viewpoint of structural chemistry, since it can assume different conformations due to intramolecular rotation along the single C–C and C–O bonds, as well as exhibit different tautomers. Previous *ab initio* molecular orbital calculations on monomeric pyruvic acid[11,18–20] predicted the existence of four conformers, all exhibiting a planar heavy-atom framework with two methyl hydrogens symmetrically situated with respect to the molecular plane (Fig. 1).

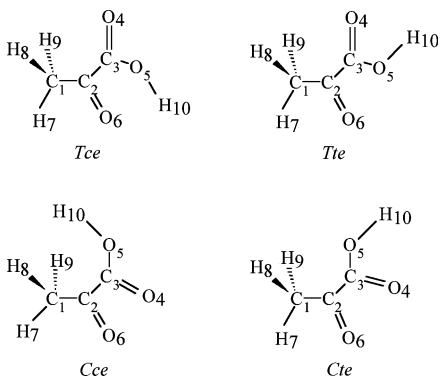


**Fig. 1** Conformers of pyruvic acid and atom numbering scheme.

These calculations had found conformer *Tce* (Fig. 1) to be the lowest energy structure.[11,18–23] *Cte* and *Tte* species were predicted to have higher energies than *Tce* within the range 0.5–3 kcal $mol^{-1}$, depending on the level of calculation.[11] In relation to experiment, this energy difference means that conformers *Tte* and *Cte*, along with *Tce*, could be present in the gas-phase pyruvic acid in noticeable amounts. The fourth possible conformer, *Cce*, was predicted to have a much higher energy (from 10.3 to 12.8 kcal $mol^{-1}$ above *Tce*[11]).

*Department of Chemistry, University of Delhi, Delhi, 110 007, India. E-mail: rita_kakkar@vsnl.com*

 

Several microwave studies of gaseous pyruvic acid have been reported.[24–26] In consonance with the theoretical predictions, the main conclusion from these studies is that the most stable conformation is *Tce*. No other conformers have been experimentally found by this method. On the other hand, infrared studies of gaseous pyruvic acid[27] revealed the existence of two pyruvic acid forms at temperatures between 363 and 453 K. The most stable *Tce* conformer could be easily identified spectroscopically due to the observation of the low-frequency O–H and C=O stretching bands associated with the intramolecularly hydrogen-bonded groups in this form (see Fig. 1). The precise nature of the second conformer could not be established, although it has been proposed that the conformation adopted by the hydroxyl group is with all probability *trans* (*i.e.*, the second observed conformer could be either *Tte* or *Cte*). In a matrix isolation infrared study of sixteen isotopic modifications of pyruvic acid,[28] an assignment was proposed for the vibrational spectra of all isotopic species, assuming that only the *Tce* conformer contributes to the observed spectroscopic features. However, the possibility of the presence of a small amount of another pyruvic acid conformer was not excluded. The authors also mention the presence of detectable amounts of impurities in all the samples, such as water, carbon dioxide and acetic acid.

Reva *et al.*[19] investigated the molecular structure of pyruvic acid by matrix isolation FTIR spectroscopy, density functional theory (DFT), and *ab initio* calculations. They used the calculated harmonic frequencies and IR intensities to assist the assignment of the observed bands to the different forms. They found two conformers, both of which exhibit a planar framework with the carbonyl bonds in a *trans* arrangement, but differing in the orientation of the hydroxyl hydrogen, *i.e.*, the *Tte* and *Tce* forms.

Several conformations for its enol tautomer are also possible, differing in the orientations of the hydrogen. These are also investigated, as are other possible forms, including the enantiomeric lactone forms. For all these structures, we have also calculated the vibrational frequencies, and compared with experimental data or other calculations, wherever available.

## Computational details

The DFT method was used to estimate the relative conformational stabilities and the harmonic vibrational frequencies. The calculations were performed with the B3LYP three-parameter density functional, which includes Becke's gradient exchange correction,[29] the Lee–Yang–Parr correlation functional,[30] and the Vosko–Wilk–Nusair correlation functional.[31]

Initially, the geometries of all pyruvic acid conformers were fully optimized at the B3LYP/6-31G(d) level. This was followed by harmonic frequency calculations at this level. The calculated harmonic frequencies were scaled down with the scaling factor of 0.9614 recommended by Scott and Radom[32] and were used to confirm the nature of all stationary point structures and to account for the zero-point vibrational energy contribution, which was scaled down by a factor of 0.9806. The relative stabilities of the pyruvic acid conformers were then calculated at the B3LYP/6-311 + + G(3df,3pd) level of theory for the geometries optimized at the B3LYP/6-31G(d) level. The SCF = Tight option was used in these calculations, performed using Gaussian 03 Revision B.5.[33]

In this work, we follow the nomenclature used for pyruvic acid conformers,[11,19,20] which named conformers according to the $C_{methyl}C_{keto}C_{acid}O_{hydroxyl}$ and $C_{keto}C_{acid}OH$ angles. The upper-case letter (*C*, *cis*; *T*, *trans*) refers to the CCCO dihedral angle; the lower-case letter (*c* or *t*) refers to the CCOH dihedral angle. An additional mirror set of four conformations can also be obtained by changing the orientation of the methyl group from the eclipsed to the staggered position.[21–23] The final *e* refers to the eclipsed conformation. We have also considered the four staggered conformations in the present study. Although Yang *et al.*[20] have recently calculated the relative energies and vibrational frequencies of pyruvic acid conformers at the B3LYP/6-311 + + G(3df,3pd) level, they have not done a complete study of all possible forms. In the present calculations, we have performed geometry optimizations at a lower level (B3LYP/6-31G(d)), but single point calculations at the optimized geometries at the B3LYP/6-311 + + G(3df,3pd) level have been performed to evaluate the relative energies. Moreover, we have considered all possible forms of the molecule, including the enol tautomers. We propose to show that geometry optimizations at the B3LYP/6-31G(d) level reproduce the experimental geometries adequately.

All transition states were characterized by the existence of only one imaginary frequency for motion along the reaction coordinate. Furthermore, Intrinsic Reaction Coordinate (IRC) calculations were performed to confirm that the predicted transition state structures connect the relevant reactants and products.

## Results and discussion

### Relative energy of conformers

All four pyruvic acid eclipsed conformers (Fig. 1) were first investigated. In agreement with previous calculations, the *Tce* conformer was found to be the most stable (see Table 1). The relative energies of the eclipsed conformers follow the order *Tce* < *Tte* < *Cte* < *Cce*. The small difference in energies between the first three conformers implies that all three are in equilibrium

**Table 1** Calculated relative energies (kcal mol$^{-1}$) of the various forms[b] of pyruvic acid at the B3LYP/6-311 + + G(3df,3pd)//B3LYP/6-31G(d) level

| System | Energy[a] |
|---|---|
| *Tce* | 0.0 |
| *Tte* | 2.6 (2.6) |
| *Cce* | 10.3 (10.4) |
| *Cte* | 4.2 (4.1) |
| *Tcs* | 0.8 (0.7) |
| *Tts* | 3.5 (3.4) |
| *Ccs* | 11.9 |
| *Cts* | 5.4 (5.3) |
| *Enol-a* | 11.1 |
| *Enol-b* | 19.7 |
| *Enol-c* | 11.1 |
| *Enol-d* | 8.4 |
| *Enol-e* | 17.3 |
| *Enol-f* | 9.9 |
| *Enol-g* | 11.4 |
| *Enol-h* | 5.9 |
| *La* | 30.8 |
| *Lb* | 29.3 |

[a] The zero-point corrected energy of *Tce* is −342.4690724 Hartree. Values in parentheses are the B3LYP/6-311 + + G(3df,3pd) results from ref. 20. [b] See Fig. 1.

in the ground state of pyruvic acid. The agreement between the present results and those calculated at the B3LYP/6-311 + + G(3df,3pd)//B3LYP/6-311 + + G(3df,3pd) level is good.

Tables 2 and 3 present the optimized geometries of the four eclipsed conformational states (*Tce*, *Tte*, *Cce* and *Cte*) of pyruvic acid calculated at the B3LYP/6-31G(d) level, their predicted rotational constants and dipole moments. Experimental data[24,25] for the most stable *Tce* conformer are also included in Table 2 for comparison. Good agreement can be seen with the previously calculated and experimental geometries. However, as in the calculations of Yang *et al.*,[20] the optimized C–C bond lengths are slightly larger than the experimental ones. The standard deviation of the calculated bond lengths from the experimental ones for *Tce* is found to be 1.2%. The experimental determinations failed to locate the *Cce* conformer. The calculated values for the standard deviations from the experimental values for the *Tte*, *Cce* and *Cte* conformers are 1.4%, 2.0% and 1.7%. These increases are of the same order as the decreases in stability, confirming that *Tce* is the preferred conformer, with contributions from *Tte* and *Cte*, as the difference in relative energies is small.

The present calculation is in good agreement with all the earlier studies,[11,19–23] which affirms the validity of the present computational method. In contrast to more involved HF and MP2 calculations[19] that did not show convergence for the *Cce* conformer, the present DFT calculations show that the corresponding total energy converges at 10.3 kcal mol$^{-1}$ above the *Tce* minimum. The agreement with the B3LYP/6-311 + + G(3df,3pd)//B3LYP/6-311 + + G(3df,3pd) results,[20] in particular, is within ±0.1 kcal mol$^{-1}$, indicating that for large systems, B3LYP/6-311 + + G(3df,3pd)//B3LYP/6-31G(d) is a better option, since the energy is quite insensitive to the quality of the geometry.[34–36]

**Table 2** Optimized geometrical parameters,[d] observed and theoretical rotational constants (*A*, *B*, *C*) and dipole moment ($\mu$) of the pyruvic acid conformer *Tce*

| | Present | Other[a] | MP2[a] | Expt.[b,c] |
|---|---|---|---|---|
| $C_2C_1$/Å | 1.499 | 1.496 | 1.499 | 1.486 |
| $C_3C_2$/Å | 1.549 | 1.552 | 1.545 | 1.523 |
| $O_4C_3$/Å | 1.207 | 1.198 | 1.218 | 1.215 |
| $O_5C_3$/Å | 1.338 | 1.332 | 1.347 | 1.328 |
| $O_6C_2$/Å | 1.219 | 1.209 | 1.233 | 1.231 |
| $H_7C_1$/Å | 1.091 | 1.086 | 1.096 | 1.074 |
| $H_8C_1$/Å | 1.096 | 1.091 | 1.101 | 1.106 |
| $H_9C_1$/Å | 1.096 | 1.091 | 1.101 | 1.106 |
| $H_{10}O_5$/Å | 0.983 | 0.974 | 0.980 | 0.983 |
| $C_3C_2C_1$/° | 117.2 | 117.0 | 117.0 | 118.6 |
| $O_4C_3C_2$/° | 123.1 | 123.1 | 123.0 | 122.0 |
| $O_5C_3C_2$/° | 112.3 | 112.7 | 113.0 | 114.5 |
| $O_6C_2C_1$/° | 125.3 | 125.3 | 125.2 | 125.0 |
| $H_7C_1C_2$/° | 110.1 | 110.1 | 109.8 | 110.7 |
| $H_8C_1C_2$/° | 109.8 | 109.6 | 109.2 | 109.0 |
| $H_9C_1C_2$/° | 109.8 | 109.6 | 109.2 | 109.0 |
| $H_{10}O_5C_3$/° | 106.1 | 107.1 | 105.6 | 105.2 |
| $O_4C_3C_2C_1$/° | 0.0 | 0.0 | 0.0 | — |
| $O_5C_3C_2C_1$/° | 180.0 | 180.0 | 180.0 | — |
| $O_6C_2C_1C_3$/° | 180.0 | 180.0 | 180.0 | — |
| $H_7C_1C_2C_3$/° | 180.0 | 180.0 | 180.0 | — |
| $H_8C_1C_2O_6$/° | 121.9 | 122.0 | 121.9 | — |
| $H_9C_1C_2O_6$/° | −121.9 | −122.0 | −121.9 | — |
| $H_{10}O_5C_3O_2$/° | 0.0 | 0.0 | 0.0 | — |
| $A$/cm$^{-1}$ | 0.183 | — | 0.181 | 0.185 |
| $B$/cm$^{-1}$ | 0.119 | — | 0.119 | 0.120 |
| $C$/cm$^{-1}$ | 0.073 | — | 0.073 | 0.074 |
| $\mu$/debye | 2.44 | 2.38 | 2.63 | 2.30 |

[a] Calculated geometry from ref. 20. [b] Experimental geometry from ref. 24. [c] Experimental rotational constants and dipole moments from ref. 25. [d] See Fig. 1.

The pyruvic acid molecule is stabilized by hydrogen bonding in the condensed phase.[37] Localized orbital studies of hydrogen bonding on the pyruvic acid molecule,[38] however, revealed that the intramolecular hydrogen bonding in the *Tce* isomer of pyruvic acid is weak due to geometric restrictions on the $O_6 \cdots H_{10}$–$O_5$ bond angle. This explains the negligible stabilization of *Tce* relative to *Tte*.

On the basis of the literature on formates and acetates, the energy differences among the pyruvic acid conformers may be considered in terms of dipole alignment of the carbonyl bonds[39] and possible contributions from steric, conjugation, and aromaticity effects.[40,41] The calculated molecular dipole moments for the *cis* isomers (*Cce*: 5.57 D, *Cte*: 4.09 D, see Table 3), in which the carbonyl bond dipoles are parallel and hence reinforce each other (Fig. 1), are higher than the corresponding values for the *trans* isomers (*Tce*: 2.44 D, *Tte*: 1.30 D, see Tables 2 and 3), in which the dipoles oppose each other. The relative stability order clearly agrees with the finding[39] that the conformer with the smaller dipole moment is always more stable.

Theoretical studies[19–23] also analyzed in detail the exact equilibrium arrangement of the methyl group in pyruvic acid. We also calculated the energies of the corresponding staggered forms. All the staggered structures were found to have a higher total energy than the corresponding eclipsed forms (see Table 1). As found for other molecules bearing a methyl group adjacent to a carbonyl (*e.g.*, acetic and thioacetic acids, acetone, acetaldehyde,[42–44] it is now well established that, in pyruvic acid, the methyl group assumes a conformation where one of the hydrogen atoms is synperiplanar with respect to the carbonyl oxygen.

## Other tautomers

**Enol tautomer.** We also considered the enol tautomer of pyruvic acid. This is important, as the direct decarboxylation to vinyl alcohol would involve this tautomer. Several conformers of this tautomer are possible, too, and these are depicted in Fig. 2. Our calculations suggest that the preferred conformer is *h*, but the differences in energy are extremely small. This is found to be less stable than the *Tce* form by 6 kcal mol$^{-1}$. The relative stabilities of the eight conformers are given in Table 1 and their optimized geometries are given in Table 4. Except *e*, all are planar.

**Enantiomeric lactone-type isomers.** Two rotamers of the lactone form were considered; these are depicted in Fig. 3 and the optimized geometries are given in Table 5. Despite the presence of strained three-membered C–C–O rings, the two lactone conformers are found to be stable. The *b* conformer is found to be more stable (see Table 1). Table 5 also gives the geometry calculated at the SCF/6-311G** level[19] for this conformer.

## Vibrational spectra

Recently, it has been proved[19] unequivocally that, besides the more stable *Tce* conformer, the *Tte* conformer is also present in equilibrium. Tables 6 and 7 compare the calculated vibrational frequencies with the experimental frequencies and those calculated

**Table 3** Optimized geometrical parameters,[b] theoretical rotational constants ($A$, $B$, $C$) and dipole moments ($\mu$) of the pyruvic acid conformers *Tte*, *Cce* and *Cte*

| | *Tte* | | *Cce* | | *Cte* | |
|---|---|---|---|---|---|---|
| | Present | Other[a] | Present | Other[a] | Present | Other[a] |
| $C_2C_1$/Å | 1.508 | 1.501 | 1.519 | 1.513 | 1.510 | 1.503 |
| $C_3C_2$/Å | 1.547 | 1.551 | 1.563 | 1.567 | 1.552 | 1.558 |
| $O_4C_3$/Å | 1.212 | 1.201 | 1.199 | 1.197 | 1.204 | 1.199 |
| $O_5C_3$/Å | 1.342 | 1.336 | 1.358 | 1.354 | 1.355 | 1.351 |
| $O_6C_2$/Å | 1.210 | 1.203 | 1.207 | 1.189 | 1.209 | 1.194 |
| $H_7C_1$/Å | 1.091 | 1.086 | 1.091 | 1.086 | 1.092 | 1.086 |
| $H_8C_1$/Å | 1.096 | 1.091 | 1.099 | 1.093 | 1.096 | 1.091 |
| $H_9C_1$/Å | 1.096 | 1.091 | 1.099 | 1.093 | 1.096 | 1.091 |
| $H_{10}O_5$/Å | 0.976 | 0.969 | 0.970 | 0.963 | 0.977 | 0.969 |
| $C_3C_2C_1$/° | 114.6 | 114.7 | 119.0 | 118.8 | 118.0 | 117.9 |
| $O_4C_3C_2$/° | 123.1 | 124.9 | 121.8 | 123.0 | 124.1 | 124.3 |
| $O_5C_3C_2$/° | 112.4 | 112.6 | 116.8 | 116.5 | 111.7 | 111.7 |
| $O_6C_2C_1$/° | 124.8 | 122.8 | 122.9 | 122.2 | 124.3 | 124.2 |
| $H_7C_1C_2$/° | 109.4 | 109.5 | 109.0 | 109.2 | 109.3 | 109.4 |
| $H_8C_1C_2$/° | 110.2 | 110.0 | 111.2 | 110.9 | 110.4 | 110.2 |
| $H_9C_1C_2$/° | 110.2 | 110.0 | 111.2 | 110.9 | 110.4 | 110.2 |
| $H_{10}O_5C_3$/° | 106.4 | 107.5 | 111.4 | 111.9 | 106.6 | 107.5 |
| $O_4C_3C_2C_1$/° | 0.0 | 0.0 | 180.0 | 180.0 | 180.0 | 180.0 |
| $O_5C_3C_2C_1$/° | 180.0 | 180.0 | 0.0 | 0.0 | 0.0 | 0.0 |
| $O_6C_2C_1C_3$/° | 180.0 | 180.0 | 180.0 | 180.0 | 180.0 | 180.0 |
| $H_7C_1C_2C_3$/° | 180.0 | 180.0 | 180.0 | 180.0 | 180.0 | 180.0 |
| $H_8C_1C_2O_6$/° | 121.5 | 121.7 | 119.7 | 120.0 | 121.2 | 121.4 |
| $H_9C_1C_2O_6$/° | −121.5 | −121.7 | −119.7 | −120.0 | −121.3 | −121.4 |
| $H_{10}O_5C_3C_2$/° | 180.0 | 180.0 | 0.0 | 0.0 | 180.0 | 180.0 |
| $A$/cm$^{-1}$ | 0.187 | — | 0.182 | — | 0.184 | — |
| $B$/cm$^{-1}$ | 0.115 | — | 0.115 | — | 0.116 | — |
| $C$/cm$^{-1}$ | 0.072 | — | 0.071 | — | 0.072 | — |
| $\mu$/debye | 1.30 | 1.27 | 5.57 | 5.51 | 4.09 | 4.06 |

[a] From ref. 20. [b] See Fig. 1.

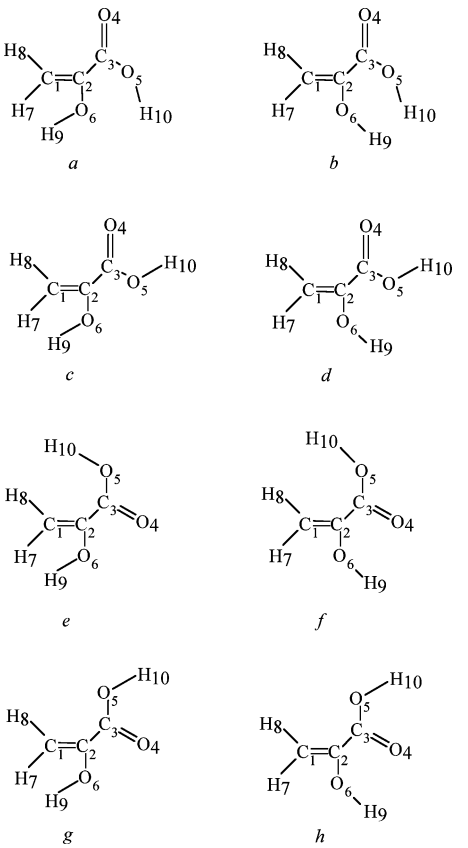


**Fig. 2** Conformers of the enol form.

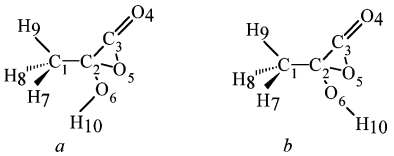


**Fig. 3** Conformers of the lactone forms.

by other methods[19,20] for these two conformers. Reasonable agreement with the experimental vibrational frequencies can be seen. The agreement with experimental frequencies is better than that obtained by other authors, validating our calculation method. Most of the bands that were not observed experimentally[19] are the ones calculated with low intensity. Note the slightly smaller values of the O–H stretch frequency for *Tce* (3432 cm$^{-1}$ compared to 3556 cm$^{-1}$ in *Tte*) and the carbonyl stretch frequency (1728 cm$^{-1}$ instead of 1764 cm$^{-1}$ in *Tte*), both on account of weak intramolecular hydrogen bonding in *Tce* (see Tables 6 and 7). The *Cce* conformer, as well as all the four staggered conformers, have imaginary frequencies, signifying that they are not energy minima. Thus the only important conformers are *Tce*, *Tte* and *Cte*, and this in agreement with calculations with larger basis sets.[19,20] All of the staggered forms possess one imaginary frequency, signifying that they are not energy minima on the potential energy surface.

In the case of the enol tautomers, the *b* conformer has two imaginary vibrational frequencies, indicating that this is not an equilibrium structure. The close proximity of hydrogens $H_9$ and

**Table 4** Optimized geometrical parameters,[a] theoretical rotational constants ($A$, $B$, $C$,) and dipole moments ($\mu$) of the enol forms of pyruvic acid

| | *a* | *b* | *c* | *d* | *e* | *f* | *g* | *h* |
|---|---|---|---|---|---|---|---|---|
| $C_2C_1$/Å | 1.334 | 1.338 | 1.339 | 1.338 | 1.342 | 1.341 | 1.340 | 1.339 |
| $C_3C_2$/Å | 1.506 | 1.508 | 1.498 | 1.493 | 1.512 | 1.506 | 1.497 | 1.490 |
| $O_4C_3$/Å | 1.207 | 1.206 | 1.213 | 1.209 | 1.203 | 1.215 | 1.210 | 1.220 |
| $O_5C_3$/Å | 1.350 | 1.365 | 1.350 | 1.366 | 1.358 | 1.343 | 1.357 | 1.345 |
| $O_6C_2$/Å | 1.376 | 1.377 | 1.363 | 1.364 | 1.355 | 1.351 | 1.360 | 1.357 |
| $H_7C_1$/Å | 1.086 | 1.084 | 1.086 | 1.084 | 1.087 | 1.084 | 1.087 | 1.084 |
| $H_8C_1$/Å | 1.082 | 1.081 | 1.082 | 1.082 | 1.084 | 1.084 | 1.081 | 1.082 |
| $H_9O_6$/Å | 0.970 | 0.965 | 0.971 | 0.971 | 0.971 | 0.981 | 0.971 | 0.978 |
| $H_{10}O_5$/Å | 0.975 | 0.969 | 0.976 | 0.975 | 0.972 | 0.971 | 0.975 | 0.976 |
| $C_3C_2C_1$/° | 121.9 | 118.6 | 119.7 | 120.1 | 122.8 | 125.8 | 123.2 | 124.0 |
| $O_4C_3C_2$/° | 123.2 | 122.4 | 124.1 | 126.7 | 123.3 | 119.3 | 124.6 | 121.3 |
| $O_5C_3C_2$/° | 114.7 | 119.0 | 112.7 | 110.5 | 115.2 | 119.8 | 112.4 | 115.3 |
| $O_6C_2C_3$/° | 111.7 | 122.6 | 113.8 | 117.5 | 111.0 | 111.8 | 110.6 | 112.6 |
| $H_7C_1C_2$/° | 122.5 | 120.6 | 122.0 | 120.9 | 122.0 | 120.4 | 121.6 | 120.6 |
| $H_8C_1C_2$/° | 118.9 | 119.7 | 119.5 | 119.5 | 121.3 | 123.0 | 120.6 | 120.4 |
| $H_9O_6C_2$/° | 110.2 | 113.3 | 108.5 | 108.3 | 109.0 | 105.6 | 108.4 | 106.0 |
| $H_{10}O_5C_3$/° | 108.8 | 113.8 | 105.4 | 106.8 | 109.3 | 110.6 | 105.5 | 106.3 |
| $O_4C_3C_2C_1$/° | 0.0 | 0.0 | 0.0 | 0.0 | 147.3 | 180.0 | 180.0 | 180.0 |
| $O_5C_3C_2C_1$/° | 180.0 | 180.0 | 180.0 | 180.0 | −31.4 | 0.0 | 0.0 | 0.0 |
| $O_6C_2C_3O_4$/° | 180.0 | 180.0 | 180.0 | 180.0 | −30.3 | 0.0 | 0.0 | 0.0 |
| $H_7C_1C_2C_3$/° | 180.0 | 180.0 | 180.0 | 180.0 | −177.3 | 180.0 | 180.0 | 180.0 |
| $H_8C_1C_2O_6$/° | 180.0 | 180.0 | 180.0 | 180.0 | 175.5 | 180.0 | 180.0 | 180.0 |
| $H_9O_6C_2C_1$/° | 0.1 | 180.0 | 0.0 | 180.0 | −4.3 | 180.0 | 0.0 | 180.0 |
| $H_{10}O_5C_3O_4$/° | 180.0 | 180.0 | 0.0 | 0.0 | 169.6 | 180.0 | 0.0 | 0.0 |
| $A$/cm$^{-1}$ | 0.184 | 0.186 | 0.188 | 0.186 | 0.185 | 0.186 | 0.189 | 0.187 |
| $B$/cm$^{-1}$ | 0.123 | 0.117 | 0.120 | 0.121 | 0.115 | 0.122 | 0.119 | 0.122 |
| $C$/cm$^{-1}$ | 0.074 | 0.072 | 0.073 | 0.074 | 0.075 | 0.074 | 0.073 | 0.074 |
| $\mu$/debye | 5.13 | 3.47 | 2.06 | 1.67 | 5.46 | 3.09 | 2.92 | 1.81 |

[a] See Fig. 2.

**Table 5** Optimized geometrical parameters,[a] theoretical rotational constants ($A$, $B$, $C$) and dipole moments ($\mu$) of the *a* and *b* lactone forms

| | Lactone | | |
|---|---|---|---|
| | *a* | *b* | *a* (6-311G**)[b] |
| $C_2C_1$/Å | 1.503 | 1.498 | 1.500 |
| $C_3C_2$/Å | 1.461 | 1.462 | 1.437 |
| $O_4C_3$/Å | 1.196 | 1.199 | 1.163 |
| $O_5C_2$/Å | 1.583 | 1.601 | 1.300 |
| $O_6C_2$/Å | 1.357 | 1.357 | 1.347 |
| $H_7C_1$/Å | 1.098 | 1.095 | 1.081 |
| $H_8C_1$/Å | 1.095 | 1.091 | 1.087 |
| $H_9C_1$/Å | 1.091 | 1.095 | 1.084 |
| $H_{10}O_6$/Å | 0.974 | 0.972 | 0.944 |
| $C_3C_2C_1$/° | 124.1 | 124.6 | 124 |
| $O_4C_3C_2$/° | 152.4 | 151.8 | 155 |
| $O_5C_2C_1$/° | 112.3 | 112.9 | — |
| $O_6C_2C_3$/° | 117.1 | 122.4 | 117 |
| $H_7C_1C_2$/° | 110.1 | 109.4 | 111 |
| $H_8C_1C_2$/° | 109.6 | 110.8 | 110 |
| $H_9C_1C_2$/° | 111.2 | 109.5 | 110 |
| $H_{10}O_6C_2$/° | 109.4 | 110.3 | 110 |
| $O_4C_3C_2C_1$/° | 87.3 | 91.0 | 84 |
| $O_5C_3C_2C_1$/° | −87.3 | −91.2 | −95 |
| $O_6C_2C_3O_4$/° | −79.4 | −78.5 | — |
| $H_7C_1C_2C_3$/° | 135.2 | 136.7 | — |
| $H_8C_1C_2C_3$/° | −105.5 | 15.9 | — |
| $H_9C_1C_2O_3$/° | 15.1 | −104.6 | — |
| $H_{10}O_6C_2C_1$/° | 36.8 | −169.1 | — |
| $A$/cm$^{-1}$ | 0.207 | 0.208 | — |
| $B$/cm$^{-1}$ | 0.100 | 0.039 | — |
| $C$/cm$^{-1}$ | 0.090 | 0.089 | — |
| $\mu$/debye | 5.19 | 3.00 | — |

[a] See Fig. 3. [b] From ref. 19.

$H_{10}$ is responsible for the low stability of this conformer (see Fig. 2). In *e* and *g*, too, the two hydrogens, $H_7$ and $H_9$, are *syn* to each other, but the former structure is nonplanar, and the two distances are 2.314 Å and 2.357 Å, respectively, compared to 1.786 Å for *b*. Conformer *f*, too, has a small imaginary frequency.

Both the lactone conformers have all-real frequencies and are thus energy minima on the potential energy surface, although they are about 30 kcal mol$^{-1}$ above the global minimum, *Tce*.

## Unimolecular decomposition

Having obtained the stable conformations of pyruvic acid and its tautomers, we investigated its thermal unimolecular decomposition. The decarboxylation of pyruvic acid to acetaldehyde has an important biomedical role. It prevents excessive production of lactic acid resulting from excess of pyruvic acid.

Discussion of possible pathways has focused on the probability of formation of the intermediate carbene from a five-center transition state compared with direct formation of acetaldehyde and carbon dioxide, which would require a highly strained four-center transition state. While some studies favor the former pathway,[3–5] other studies suggest the latter, possibly from highly vibrationally excited ground-state molecules, and it seems likely that the reaction pathway will depend upon the photon energy.[2] According to Yamamoto and Back,[5] the UV photolysis of pyruvic acid produces carbon dioxide and hydroxyethylidene through a five-center transition state. On the other hand, in the thermal decomposition using a static system, they proposed that the reaction proceeds through a four-center transition state, which directly gives carbon dioxide and acetaldehyde.

**Table 6** Calculated,[a] experimental, other DFT and *ab initio* harmonic frequencies ($\nu$) and intensities of the pyruvic acid conformer *Tce*

| Present | | Expt.[b] | | Other[c] | | MP2[b] | |
|---|---|---|---|---|---|---|---|
| $\nu$/cm$^{-1}$ | Intensity/km mol$^{-1}$ | $\nu$/cm$^{-1}$ | Relative Intensity | $\nu$/cm$^{-1}$ | Intensity/km mol$^{-1}$ | $\nu$/cm$^{-1}$ | Intensity/km mol$^{-1}$ |
| 3420 | 98.7 | 3432 | 0.206 | 3564 | 32 | 3477 | 117.9 |
| 3057 | 5.6 | 3032 | 0.004 | 3094 | 1 | 3085 | 3.8 |
| 3003 | 0.8 | — | — | — | — | 3037 | — |
| 2947 | 0.2 | 2936 | 0.005 | — | — | 2955 | 0.4 |
| 1802 | 188.2 | 1800 | 0.646 | 1807 | 74 | 1791 | 193.2 |
| 1733 | 99.4 | 1728 | 0.212 | 1749 | 32 | 1715 | 65.3 |
| 1427 | 10.9 | 1424 | 0.051 | 1427 | 4 | 1439 | 10.2 |
| 1425 | 13.4 | 1408 | 0.014 | — | — | 1431 | 11.7 |
| 1375 | 125.9 | 1385 | 0.162 | 1374 | 2 | 1397 | 92.8 |
| 1355 | 269.8 | 1355 | 0.946 | 1349 | 100 | 1357 | 221.8 |
| 1214 | 83.5 | 1214 | 0.495 | 1218 | 24 | 1245 | 105.0 |
| 1127 | 65.4 | 1137 | 0.143 | 1133 | 19 | 1139 | 55.4 |
| 1000 | 2.8 | 1018 | 0.027 | — | — | 1015 | 1.0 |
| 951 | 14.8 | 968 | 0.121 | 981 | 6 | 969 | 13.8 |
| 741 | 8.7 | 762 | 0.045 | 766 | 2 | 730 | 27.0 |
| 724 | 57.5 | 664 | 0.490 | 742 | 5 | 686 | 65.9 |
| 664 | 5.7 | 653 | 0.021 | 704 | 23 | — | — |
| 584 | 16.6 | 604 | 0.118 | 610 | 5 | 596 | 16.4 |
| 508 | 2.9 | 535 | vw | 525 | 1 | 521 | 3.0 |
| 385 | 12.4 | 395 | — | 399 | 5 | 386 | 15.7 |
| 376 | 17.2 | 388 | — | 391 | 3 | 384 | 9.4 |
| 246 | 24.0 | 258 | — | 253 | 7 | 246 | 24.3 |
| 114 | 1.4 | 134 | — | — | — | 135 | 0.1 |
| 87 | 6.0 | 124 | — | 90 | 2 | 94 | 7.0 |

[a] Scaled by 0.9614. [b] From ref. 19. Bands <400 cm$^{-1}$ were not assigned in the experimental work. MP2/aug-cc-pVDZ. [c] From ref. 20.

**Table 7** Calculated,[a] experimental, other DFT and *ab initio* harmonic frequencies ($\nu$) and intensities of the pyruvic acid conformer *Tte*

| Present | | Expt.[b] | | Other[c] | | MP2[b] | |
|---|---|---|---|---|---|---|---|
| $\nu$/cm$^{-1}$ | Intensity/km mol$^{-1}$ | $\nu$/cm$^{-1}$ | Relative Intensity | $\nu$/cm$^{-1}$ | Intensity/km mol$^{-1}$ | $\nu$/cm$^{-1}$ | Intensity/km mol$^{-1}$ |
| 3541 | 56.5 | 3556 | 0.040 | 3674 | 30 | 3582 | 89.7 |
| 3055 | 6.7 | — | — | 3093 | 2 | 3083 | 4.2 |
| 3002 | 2.8 | — | — | 3037 | 1 | 3037 | 1.6 |
| 2946 | 0.1 | — | — | — | — | 2954 | 0.2 |
| 1763 | 43.5 | 1764 | 0.126 | 1778 | 68 | 1756 | 209.4 |
| 1759 | 304.8 | 1751 | 0.138 | 1765 | 100 | 1730 | 102.8 |
| 1433 | 9.8 | — | — | 1433 | 4 | 1442 | 9.5 |
| 1429 | 12.7 | — | — | 1430 | 6 | 1432 | 12.0 |
| 1367 | 6.8 | — | — | 1370 | 4 | 1397 | 4.3 |
| 1346 | 37.8 | — | — | 1347 | 16 | 1355 | 46.0 |
| 1190 | 34.6 | — | — | 1194 | 12 | 1221 | 26.3 |
| 1112 | 230.9 | 1119 | 0.077 | 1118 | 9 | 1124 | 236.4 |
| 1006 | 2.4 | — | — | 1042 | 1 | 1015 | 1.0 |
| 943 | 35.6 | 962 | 0.023 | 971 | 18 | 963 | 33.9 |
| 715 | 14.0 | 723 | vw | 739 | 5 | 741 | 4.6 |
| 705 | 60.2 | 716 | vw | 736 | 17 | 714 | 39.1 |
| 616 | 83.8 | 588 | 0.088 | 624 | 35 | 627 | 86.2 |
| 570 | 78.1 | 592 | 0.062 | 597 | 30 | 582 | 75.5 |
| 496 | 1.8 | — | — | 514 | 1 | 511 | 1.9 |
| 374 | 1.1 | — | — | — | — | 383 | 0.9 |
| 364 | 0.0 | — | — | — | — | 375 | 0.2 |
| 239 | 9.1 | — | — | 249 | 4 | 243 | 9.1 |
| 120 | 0.0 | — | — | — | — | 143 | 0.0 |
| 45 | 6.3 | — | — | 32 | 3 | 41 | 6.6 |

[a] Scaled by 0.9614. [b] From ref. 19. Bands <400 cm$^{-1}$ were not assigned in the experimental work. MP2/aug-cc-pVDZ. [c] From ref. 20.

In the assumed reaction scheme (Scheme 1), including intermediates and sequences of possible elementary conversions, three channels are considered: Channel 1 leads directly to acetaldehyde through a four-center-like transition state (TS1), Channel 2 leads to hydroxyethylidene through a five-center-like transition state (TS2), and Channel 3 leads to vinyl alcohol through a four-center transition state (TS4). In the Channel 3 case, TS4 is formed from the enol tautomer (*enol-a*). The transition state TS3 connects the higher potential energy enol tautomer to the keto form of pyruvic acid.

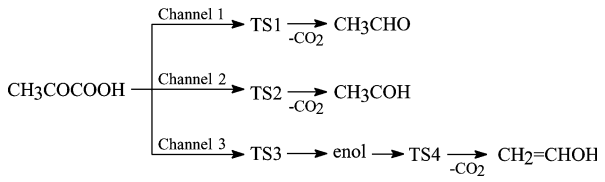


**Scheme 1**

The decarboxylation products of Channel 1 are acetaldehyde and carbon dioxide. The reaction is exothermic ($\Delta H = -11.3$ kcal mol$^{-1}$). However, this reaction has a high activation barrier of 70.1 kcal mol$^{-1}$.

The products of reaction by Channel 2 are hydroxyethylidene and carbon dioxide. Contrary to our previous results from PM3 calculations,[45] no hydroxyethylidene–carbon dioxide complex is formed. Extensive computational efforts failed to locate a transition state connecting pyruvic acid to the products. Even at the B3LYP/6-311 + + G(3df,3pd)//B3LYP/6-311 + + G(3df,3pd) level, there was no convergence of the transition state, TS2. We re-optimized the relevant structures with this higher basis set, since the products are smaller, and more amenable to higher-level calculations; the results are given in Table 8. This table reveals that in most cases the calculations at the two levels agree within ±0.1 kcal mol$^{-1}$ of each other.

Reaction by Channel 3 involves the initial transfer of a proton from pyruvic acid to give the enol tautomer, followed by the decarboxylation reaction giving vinyl alcohol and carbon dioxide. The initial enolization is itself a high-energy process. The transition state (TS3) is four-centered. The activation energy required for this process (68.5 kcal mol$^{-1}$) is only slightly smaller than that for decarboxylation, and the latter is the rate-determining step. The overall activation energy for vinyl alcohol formation is very high, *i.e.* 75.8 kcal mol$^{-1}$.

Previous investigations of the decomposition have been carried out using static systems. Yamamoto and Back[5] proposed that initiation by UV photolysis involves fragmentation into carbon dioxide and hydroxyethylidene. On the other hand, they assumed that the thermal decomposition gave acetaldehyde through a four-center transition state directly instead of the carbene. Taylor[46] proposed, for the thermal reactions of a series of substituted compounds of pyruvic acid, that the decomposition also proceeds through a four-center transition state to give carbon dioxide and aldehydes. He also explained the relative decomposition rates of these compounds as being due to charge-induced effects. His proposal was reasonable since the relative reactivity showed a linear correlation using the Hammett rule. Therefore, the previous two research groups concluded that the initial process in the thermal decomposition produced aldehyde directly. Our results are in perfect agreement with these experiments as the path leading to hydroxyethylidene simply does not exist.

## NBO analysis

The results reported in the previous sections prove emphatically that acetaldehyde is formed directly from pyruvic acid *via* TS1. However, some previous lower-level theoretical studies had reported that the preferred product is a hydroxyethylidene–carbon dioxide complex through the transition state TS2.[45,47] To investigate the question of why the present, more rigorous calculations do not lead to this transition state, we have carried out an NBO analysis of the *Tce* and TS1 structures. Moreover, the higher stability of the eclipsed conformations of pyruvic acid over the staggered ones has also been ascribed to more favorable $\pi(CH_3) \rightarrow \pi^*(C{=}O)$ group orbital interactions and hyperconjugation through the σ bond system.[23,42] The NBO method[48] was used to identify the best Lewis structure representations of the equilibrium geometries and to determine the transformation of the reactant Lewis structures into that of the products.

Tables 9 and 10 give the results of the calculations. Lewis structures are found to account for 98.4% of the bonding in *Tce*. However, hyperconjugation through the σ bond system including $C_1H_7$, $C_3O_4$, $O_5H_{10}$, and in-plane oxygen (particularly $O_4$) cores and lone pairs weakens the $C_2C_3$ bond by putting 0.13 electrons in the corresponding σ* orbital. The interaction with the $O_5H_{10}$ bond favors migration of $H_{10}$ to $C_2$, but not to $O_6$, with which it has no interaction. This agrees with localized orbital calculations,[38] which had indicated weak intramolecular hydrogen bonding in pyruvic acid because of geometric restrictions. The optimized $O_6 \cdots H_{10}$ distance of 2 Å is also rather long and indicates a weak hydrogen bonding interaction.

The $C_3O_4$ π bond is also weakened by conjugation with the out-of-plane $O_5$ lone pair and the $C_2O_6$ π-bond, particularly the former, which puts 0.21 electrons into the corresponding π* orbital.

For the transition state, the contribution of Lewis structures reduces to 96.2%. This is because the migrating hydrogen atom transfers electron density to both the $C_2C_3$ σ* orbital and the $C_3O_4$ π* orbitals, as in pyruvic acid, but to a much larger extent, particularly to the former (0.43 electrons). Table 10 indicates that the $C_2C_3$ σ bond becomes polar, the electron pair moving towards $C_2$. The corresponding σ* orbital is concentrated at $C_3$.

**Table 8** Relative energies (kcal mol$^{-1}$) of the various structures on the potential energy surface at the B3LYP/6-311 + + G(3df,3pd)//B3LYP/6-31G(d) and the B3LYP/6-311 + + G(3df,3pd)//B3LYP/6-311 + + G(3df,3pd) levels

| Structure | B3LYP/6-311 + + G(3df,3pd)//B3LYP/6-31G(d) | B3LYP/6-311 + + G(3df,3pd)//B3LYP/6-311 + + G(3df,3pd) |
|---|---|---|
| Pyruvic acid | 0.0[a] | 0.0[b] |
| TS1 | 70.1 | 70.1 |
| *Trans*-hydroxyethylidene + $CO_2$ | 39.6 | 39.5 |
| Vinyl alcohol + $CO_2$ | −1.1 | −1.1 |
| Acetaldehyde + $CO_2$ | −11.3 | −11.4 |
| TS5 + $CO_2$ | 68.0 | 67.8 |
| TS6 + $CO_2$ | 61.3 | 61.3 |
| TS7 + $CO_2$ | 54.3 | 54.2 |

[a] Zero-point corrected energy = −342.469072 Hartree. [b] Zero-point corrected energy = −342.468619 Hartree.

**Table 9** NBO analysis of pyruvic acid

| NLMO | Occupancy | Orbital | Center | % | Hybrid |
|---|---|---|---|---|---|
| 1 | 2.00 | $\sigma(C_2–O_6)$ | $C_2$ | 34.19 | $sp^{2.18}$ |
| | | | $O_6$ | 65.81 | $sp^{1.38}$ |
| 2 | 2.00 | $\sigma(C_3–O_4)$ | $C_3$ | 35.21 | $sp^{1.81}$ |
| | | | $O_4$ | 64.79 | $sp^{1.47}$ |
| 3 | 2.00 | $\sigma(C_3–O_5)$ | $C_3$ | 32.43 | $sp^{2.41}$ |
| | | | $O_5$ | 67.57 | $sp^{2.08}$ |
| 4 | 1.98 | $\sigma(O_5–H_{10})$ | $O_5$ | 75.94 | $sp^{3.63}$ |
| | | | $H_{10}$ | 24.06 | s |
| 5 | 1.98 | $n_1(O_6)$ | $O_6$ | 100 | $sp^{0.73}$ |
| 6 | 1.98 | $n_1(O_4)$ | $O_4$ | 100 | $sp^{0.68}$ |
| 7 | 1.99 | $\sigma(C_1–C_2)$ | $C_1$ | 50.04 | $sp^{2.60}d^{0.01}$ |
| | | | $C_2$ | 49.96 | $sp^{1.61}$ |
| 8 | 1.98 | $\sigma(C_2–C_3)$ | $C_2$ | 50.34 | $sp^{2.26}$ |
| | | | $C_3$ | 49.66 | $sp^{1.83}$ |
| 9 | 1.98 | $n_1(O_5)$ | $O_5$ | 100 | $sp^{1.17}$ |
| 10 | 1.99 | $\sigma(C_1–H_7)$ | $C_1$ | 61.32 | $sp^{2.98}f^{0.01}$ |
| | | | $H_7$ | 38.68 | s |
| 11 | 1.96 | $\sigma(C_1–H_8)$ | $C_1$ | 61.77 | $sp^{3.23}d^{0.01}$ |
| | | | $H_8$ | 38.23 | s |
| 12 | 1.96 | $\sigma(C_1–H_9)$ | $C_1$ | 61.77 | $sp^{3.23}d^{0.01}$ |
| | | | $H_9$ | 38.23 | s |
| 13 | 1.97 | $\pi(C_2–O_6)$ | $C_2$ | 32.57 | p |
| | | | $O_6$ | 67.53 | p |
| 14 | 1.97 | $\pi(C_3–O_4)$ | $C_3$ | 31.63 | p |
| | | | $O_4$ | 68.37 | p |
| 15 | 1.80 | $n_2(O_5)$ | $O_5$ | 100 | p |
| 16 | 1.88 | $n_2(O_6)$ | $O_6$ | 100 | p |
| 17 | 1.85 | $n_2(O_4)$ | $O_4$ | 100 | p |
| 18 | 0.21 | $\pi^*(C_3–O_4)$ | $C_3$ | 68.37 | p |
| | | | $O_4$ | 31.63 | p |
| 19 | 0.13 | $\sigma^*(C_2–C_3)$ | $C_2$ | 49.66 | $sp^{2.26}$ |
| | | | $C_3$ | 50.34 | $sp^{1.83}$ |

**Table 10** NBO analysis of the transition state for the pyruvic acid dissociation to acetaldehyde and carbon dioxide

| NLMO | Occupancy | Orbital | Center | % | Hybrid |
|---|---|---|---|---|---|
| 1 | 2.00 | $\sigma(C_2–O_6)$ | $C_2$ | 33.13 | $sp^{2.08}$ |
| | | | $O_6$ | 66.87 | $sp^{1.31}$ |
| 2 | 1.99 | $\sigma(C_3–O_4)$ | $C_3$ | 33.32 | $sp^{1.82}$ |
| | | | $O_4$ | 66.68 | $sp^{1.75}d^{0.01}$ |
| 3 | 1.99 | $\sigma(C_3–O_5)$ | $C_3$ | 34.52 | $sp^{1.46}$ |
| | | | $O_5$ | 65.48 | $sp^{2.08}d^{0.02}$ |
| 4 | 1.96 | $n_1(O_5)$ | $O_5$ | 100 | $sp^{1.64}$ |
| 5 | 1.98 | $n_1(O_6)$ | $O_6$ | 100 | $sp^{0.78}$ |
| 6 | 1.99 | $\sigma(C_1–C_2)$ | $C_1$ | 50.71 | $sp^{2.58}d^{0.01}$ |
| | | | $C_2$ | 49.29 | $sp^{1.45}$ |
| 7 | 1.97 | $n_1(O_4)$ | $O_4$ | 100 | $sp^{0.74}$ |
| 8 | 2.00 | $\pi(C_3–O_4)$ | $C_3$ | 27.98 | p |
| | | | $O_4$ | 72.02 | p |
| 9 | 1.97 | $\sigma(C_1–H_9)$ | $C_1$ | 60.97 | $sp^{3.27}d^{0.01}$ |
| | | | $H_9$ | 39.03 | s |
| 10 | 1.96 | $\sigma(C_1–H_8)$ | $C_1$ | 61.82 | $sp^{3.26}d^{0.01}$ |
| | | | $H_8$ | 38.18 | s |
| 11 | 1.98 | $\sigma(C_1–H_7)$ | $C_1$ | 61.44 | $sp^{2.96}$ |
| | | | $H_7$ | 38.56 | s |
| 12 | 1.66 | $\sigma(C_2–C_3)$ | $C_2$ | 63.81 | $sp^{2.70}d^{0.01}$ |
| | | | $C_3$ | 36.19 | $sp^{4.32}d^{0.01}$ |
| 13 | 1.96 | $\pi(C_2–O_6)$ | $C_2$ | 33.95 | p |
| | | | $O_6$ | 66.05 | p |
| 14 | 1.71 | $n_2(O_5)$ | $O_5$ | 100 | p |
| 15 | 1.66 | $n_3(O_5)$ | $O_5$ | 100 | p |
| 16 | 1.64 | $n_2(O_4)$ | $O_4$ | 100 | p |
| 17 | 1.84 | $n_2(O_6)$ | $O_6$ | 100 | p |
| 18 | 0.57 | | $H_{10}$ | 100 | s |
| 19 | 0.43 | $\sigma^*(C_2–C_3)$ | $C_2$ | 36.19 | $sp^{2.70}d^{0.01}$ |
| | | | $C_3$ | 63.81 | $sp^{4.32}d^{0.01}$ |
| 20 | 0.29 | $\pi^*(C_3–O_4)$ | $C_3$ | 72.02 | p |
| | | | $O_4$ | 27.98 | p |

The electron transfer lowers the energy of the $C_2C_3$ σ* orbital and aids the dissociation of this bond. Other factors that contribute to the weakening of this bond are electron transfer from the $C_2C_3$ σ bond and the oxygen lone pairs to the antibonding orbital. Likewise, the $C_3O_4$ bond is weakened by electron transfer from the $O_5$ lone pair orbitals to the π* orbital.

Thus the mechanism of acetaldehyde formation involves the transfer of electron density from the $O_5$ atom through the hydrogen $H_{10}$ to $C_2$, leading to the formation of a new $C_2H_{10}$ bond. The migrating hydrogen thus acts as a hydride ion, transferring the $O_5H_{10}$ bond pair to the electron-deficient carbon. It receives electron density from $C_3$ and the $O_5$ lone pair in this process and transfers it to $C_2$, thus forming a bond with it. The $C_3O_4O_5$ moiety, which had a total negative charge of −0.496, has to lose electron density to form the electrically neutral carbon dioxide molecule. This it does through the migrating hydrogen.

### Products of decomposition

Although the results of the previous section indicate acetaldehyde formation by Channel 1, the possibility of some vinyl alcohol formation by Channel 3 cannot be ruled out, as the difference in activation barriers for the two pathways is only 5.7 kcal mol$^{-1}$. The vinyl alcohol formed could then isomerize to its more stable isomer, acetaldehyde.

Previous *ab initio* studies[6–15] on the $C_2H_4O$ isomers predicted, among other things, that the transition structure linking hydroxyethylidene with acetaldehyde (1,2-hydrogen shift) might lie up to 25 kcal mol$^{-1}$ above that separating vinyl alcohol from acetaldehyde (1,3-hydrogen shift), in apparent conflict with some of the conclusions from the experimental studies.[3,4,16] Smith *et al.*[17] also carried out *ab initio* calculations at the Hartree–Fock (HF) level They found that hydroxyethylidene is separated by significant barriers from its lower energy isomers, acetaldehyde and vinyl alcohol. Further, they found that the transition state connecting vinyl alcohol and acetaldehyde is lower in energy than those connecting hydroxyethylidene with the other two isomers, which also does not agree with conclusions based on experimental observations.

Wesdemiotis and McLafferty[16] discussed the stability of hydroxyethylidene. It is a likely interstellar species[15] because its more stable isomer, acetaldehyde, has been identified in the interstellar medium.[49] A rationalization for the existence of distinct singlet *trans* and *cis* isomers is that partial C–OH double bond character forms a barrier to internal rotation of the OH group of 23.8 kcal mol$^{-1}$. Previous estimates[15] had put this barrier as 27.3 kcal mol$^{-1}$. *Cis*-hydroxyethylidene is less stable than the *trans* isomer by 2.4 kcal mol$^{-1}$. Calculation of the vibrational frequencies verifies that the geometries optimized for *trans*- and *cis*-$CH_3COH$ represent true minima on their respective potential energy surfaces.

The energy difference between acetaldehyde and vinyl alcohol is important, as these two molecules represent the prototypical keto–enol pair. Our calculated value of 10.2 kcal mol$^{-1}$ is in good agreement with the experimental[50] value of 10 ± 2 kcal mol$^{-1}$ and the *ab initio*[17] value of 11 kcal mol$^{-1}$.

The relative energy difference between acetaldehyde and hydroxyethylidene is also of interest. Some previous estimates have

been reported. Rosenfeld and Weiner[3] estimated a value of 60 kcal mol$^{-1}$ on the basis of an *ab initio* difference between formaldehyde and hydroxymethylene and the use of Benson additivity terms. Yadav and Goddard[15] proposed a value of 61.9 kcal mol$^{-1}$, assuming additivity of CISD/3-21G and HF/6-31G(d) results. Our calculated value (50.9 kcal mol$^{-1}$) is the same as the best *ab initio* value.[17]

The first transformation studied here was the one yielding acetaldehyde from *trans*-hydroxyethylidene. The barrier to this transformation is calculated as 28.4 kcal mol$^{-1}$, which is close to the *ab initio* estimate of 28.2 kcal mol$^{-1}$. The transition state, TS5, has a three-center-like structure, and is depicted in Fig. 4.

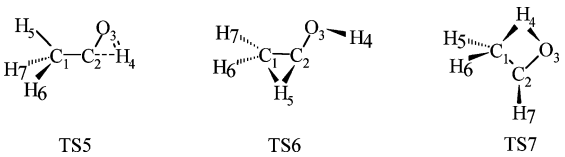


**Fig. 4** Structures of the transition states interconnecting the dissociation products.

The transition state, TS6, connecting hydroxyethylidene to vinyl alcohol also has a three-center-like structure (see Fig. 4) and the barrier to this rearrangement is 21.7 kcal mol$^{-1}$, compared to the *ab initio*[17] value of 23.4 kcal mol$^{-1}$. This is in agreement with experimental results[16] that hydroxyethylidene, despite its very high energy, should be observable, since it is separated from the lower energy isomers, acetaldehyde and vinyl alcohol, by significant barriers.

The transition state, TS7, connecting acetaldehyde to vinyl alcohol through a direct 1,3-hydrogen shift, was also examined. This barrier was calculated as 65.6 kcal mol$^{-1}$ from acetaldehyde, and the transition state has a four-center-like structure (see Fig. 4). The barrier to the reverse reaction, *i.e.* from vinyl alcohol to acetaldehyde, is 55.3 kcal mol$^{-1}$. This implies that the vinyl alcohol formed by Channel 3 could easily rearrange to acetaldehyde.

The vibrational frequencies for all the three transition states show that they are true transition states, having only one imaginary vibrational frequency.

## Discussion

Since the thermodynamically stable product is acetaldehyde, which is also the product of the enzymatic decarboxylation of pyruvic acid, we have considered its formation by two routes, *i.e.* Channel 1, involving the direct decarboxylation to acetaldehyde, and Channel 3, requiring the intermediate formation of vinyl alcohol. Experimental studies do not support the latter mechanism, as, when O-*d*-labeled pyruvic acid is used as the starting material, $CH_2DCHO$ is not observed,[16] which rules out the intermediacy of vinyl alcohol.

The alternate mechanism for the pyruvic acid decarboxylation[5,51] involves a direct intramolecular rearrangement with a four-membered cyclic transition structure (Channel 1, see Scheme 1). Our calculations support this mechanism. The calculated barrier is, however, too high (70.1 kcal mol$^{-1}$) for it to be directly operative in biological systems. As discussed earlier,[45] most biochemical reactions occur in such a way that a bond-breaking reaction is coupled with a bond-making one, so that the energy released in the former is immediately absorbed, and the release of energy does not damage the cell. Thus, decarboxylation of pyruvate occurs when it is temporarily bonded by coenzyme A, which strips a carbon dioxide molecule off pyruvate, as well as two electrons and protons which are collected by $NAD^+$, reducing it to NADH + $H^+$. The new intermediate, acetyl coenzyme A, is short-lived, and is degraded into two molecules, the original coenzyme A which is now available to bond to another pyruvate, and acetaldehyde (acetate). The enzymatic pathway thus leads to energy changes in manageable amounts. We have already seen that the $C_2$–$C_3$ bond is already weak and its dissociation is facile. It is also relatively easy for Coenzyme A to strip pyruvic acid of the acidic hydrogen, $H_{10}$.

## Conclusions

To sum up, the results of the present studies indicate:

(a) DFT calculations indicate that single-point calculations at a higher level with geometries optimized at a lower level yield good results (within ±0.1 kcal mol$^{-1}$).

(b) Contrary to expectations, there is weak hydrogen-bonding interaction in pyruvic acid.

(c) Comparison with our previous calculations with the relatively inexpensive PM3 method[45] reveals that the latter has a tendency to produce spurious intermediates on the reaction path, such as the protonated pyruvates and hydroxyethylidene–carbon dioxide complexes, and calculations using semiempirical methods are best avoided.

## Acknowledgements

Two of the authors (MP and NPR) thank the University Grants Commission (UGC) and Council of Scientific & Industrial Research (CSIR), New Delhi, for research fellowships.

## References

1 J. Berzelius, *Ann. Phys. (Weinheim, Ger.)*, 1835, **36**, 1.
2 J. A. O'Neill, T. G. Kreutz and G. W. Flynn, *J. Chem. Phys.*, 1987, **87**, 4598–4605.
3 R. N. Rosenfeld and B. Weiner, *J. Am. Chem. Soc.*, 1983, **105**, 3485–3488.
4 B. R. Weiner and R. N. Rosenfeld, *J. Org. Chem.*, 1983, **48**, 5362–5364, and references therein.
5 S. Yamamoto and R. A. Back, *Can. J. Chem.*, 1985, **63**, 549–554.
6 W. J. Bouma, D. Poppinger and L. Radom, *J. Am. Chem. Soc.*, 1977, **99**, 6443–6444.
7 W. J. Bouma, M. A. Vincent and L. Radom, *Int. J. Quantum Chem.*, 1978, **14**, 767–777.
8 V. I. Faustov and S. S. Yufit, *Russ. J. Phys. Chem. (Transl. of Zh. Fiz. Khim.)*, 1982, **56**, 1359–1361.
9 J. D. Goddard, *J. Mol. Struct. (THEOCHEM)*, 1987, **149**, 39–49.
10 J. Leska and M. Zakova, *Collect. Czech. Chem. Commun.*, 1982, **47**, 1897.
11 J. Murto, T. Raaska, H. Kunttu and M. Räsänen, *J. Mol. Struct. (THEOCHEM)*, 1989, **200**, 93–101.
12 R. A. Poirier, D. Majlessi and T. J. Zielinski, *J. Comput. Chem.*, 1986, **7**, 464–475.
13 M. Räsänen, T. Raaska, H. Kunttu and J. Murto, *J. Mol. Struct. (THEOCHEM)*, 1990, **208**, 79–90.
14 W. R. Rodwell, W. J. Bouma and L. Radom, *Int. J. Quantum Chem.*, 1980, **18**, 107–116.
15 J. S. Yadav and J. D. Goddard, *J. Chem. Phys.*, 1986, **85**, 3975–3984.
16 C. Wesdemiotis and F. W. McLafferty, *J. Am. Chem. Soc.*, 1987, **109**, 4760–4761.

 

17 B. J. Smith, M. T. Nguyen, W. J. Bouma and L. Radom, *J. Am. Chem. Soc.*, 1991, **113**, 6452–6458.
18 C. Chen and S. F. Shyu, *J. Mol. Struct. (THEOCHEM)*, 2000, **503**, 201–211.
19 D. Reva, S. G. Stepanian, L. Adamowicz and R. Fausto, *J. Phys. Chem. A*, 2001, **105**, 4773–4780.
20 X. Yang, G. Orlova, X. J. Zhou and K. T. Leung, *Chem. Phys. Lett.*, 2003, **380**, 34–41.
21 P. Tarakeshwar and S. Manogaran, *J. Mol. Struct. (THEOCHEM)*, 1998, **430**, 51–56.
22 C. van Alsenoy, C., L. Schäfer, K. Siam and J. D. Ewbank, *J. Mol. Struct. (THEOCHEM)*, 1989, **187**, 271–283.
23 Z. Y. Zhou, D. M. Du and A. P. Fu, *Vib. Spectrosc.*, 2000, **23**, 181–186.
24 C. E. Dyllick-Brenzinger, A. Bauder and Hs. H. Günthard, *Chem. Phys.*, 1977, **23**, 195–206.
25 K.-M. Marstokk and H. Møllendal, *J. Mol. Struct.*, 1974, **20**, 257–267.
26 R. Meyer and A. Bauder, *J. Mol. Spectrosc.*, 1982, **94**, 136–149.
27 A. Schellenberger, W. Beer and G. Oehme, *Spectrochim. Acta*, 1965, **21**, 1345–1351.
28 H. Hollenstein, F. Akermann and Hs. H. Günthard, *Spectrochim. Acta, Part A*, 1978, **34**, 1041–1063.
29 A. D. Becke, *Phys. Rev. A: At., Mol., Opt. Phys.*, 1988, **38**, 3098–3100.
30 C. Lee, W. Yang and R. G. Parr, *Phys. Rev. B: Condens. Matter*, 1988, **37**, 785–789.
31 S. H. Vosko, L. Wilk and M. Nusair, *Can. J. Chem.*, 1980, **58**, 1200.
32 A. P. Scott and L. Radom, *J. Phys. Chem.*, 1996, **100**, 16502–16513.
33 M. J. Frisch, G. W. Trucks, H. B. Schlegel, G. E. Scuseria, M. A. Robb, J. R. Cheeseman, J. A. Montgomery, Jr., T. Vreven, K. N. Kudin, J. C. Burant, J. M. Millam, S. S. Iyengar, J. Tomasi, V. Barone, B. Mennucci, M. Cossi, G. Scalmani, N. Rega, G. A. Petersson, H. Nakatsuji, M. Hada, M. Ehara, K. Toyota, R. Fukuda, J. Hasegawa, M. Ishida, T. Nakajima, Y. Honda, O. Kitao, H. Nakai, M. Klene, X. Li, J. E. Knox, H. P. Hratchian, J. B. Cross, C. Adamo, J. Jaramillo, R. Gomperts, R. E. Stratmann, O. Yazyev, A. J. Austin, R. Cammi, C. Pomelli, J. W. Ochterski, P. Y. Ayala, K. Morokuma, G. A. Voth, P. Salvador, J. J. Dannenberg, V. G. Zakrzewski, S. Dapprich, A. D. Daniels, M. C. Strain, O. Farkas, D. K. Malick, A. D. Rabuck, K. Raghavachari, J. B. Foresman, J. V. Ortiz, Q. Cui, A. G. Baboul, S. Clifford, J. Cioslowski, B. B. Stefanov, G. Liu, A. Liashenko, P. Piskorz, I. Komaromi, R. L. Martin, D. J. Fox, T. Keith, M. A. Al-Laham, C. Y. Peng, A. Nanayakkara, M. Challacombe, P. M. W. Gill, B. Johnson, W. Chen, M. W. Wong, C. Gonzalez and J. A. Pople, *Gaussian 03 (Revision B.5)*, Gaussian, Inc., Pittsburgh, PA, 2003.
34 P. A. Fernandes and M. J. Ramos, *J. Am. Chem. Soc.*, 2003, **125**, 6311–6322.
35 J. Stubbe and W. A. van der Donk, *Chem. Biol.*, 1995, **2**, 793–801.
36 H. Zipse, *J. Am. Chem. Soc.*, 1994, **116**, 10773–10774.
37 W. J. Ray, J. E. Katon and D. B. Philips, *J. Mol. Struct.*, 1981, **74**, 75–84.
38 M. S. Gordon and D. E. Tallman, *Chem. Phys. Lett.*, 1972, **17**, 385–392.
39 K. B. Wiberg and K. E. Laidig, *J. Am. Chem. Soc.*, 1988, **110**, 1872–1874.
40 D. M. Pawar, A. A. Khalil, D. R. Hooks, K. Collins, T. Elliot, J. Stafford, L. Smith and E. A. Noe, *J. Am. Chem. Soc.*, 1998, **120**, 2108–2112.
41 N. D. Epiotis, W. R. Cherry, S. Shaik, R. L. Yates and F. Bernardi, *Top. Curr. Chem.*, 1977, **70**, 1.
42 R. Fausto, L. A. E. Batista de Carvalho and J. J. C. Teixeira-Dias, *J. Mol. Struct. (THEOCHEM)*, 1990, **207**, 67–83.
43 D. W. Liao, A. M. Mebel, M. Hayashi, Y. J. Shiu, Y. T. Chen and S. H. Lin, *J. Chem. Phys.*, 1999, **111**, 205–215.
44 P. Nösberger, A. Bauder and Hs. H. Günthard, *Chem. Phys.*, 1973, **1**, 418.
45 R. Kakkar, P. Chadha and D. Verma, *Internet Electron. J. Mol. Des.*, 2006, **5**, in press.
46 R. Taylor, *Int. J. Chem. Kinet.*, 1991, **23**, 247–250.
47 K. Saito, G. Sasaki and S. Tanaka, *J. Phys. Chem.*, 1994, **98**, 3756–3761.
48 E. D. Glendening, A. E. Reed, J. E. Carpenter and F. Weinhold, *NBO Version 3.1*, 2001.
49 N. Fourikis, M. W. Sinclair, B. J. Robinson, P. D. Godfrey and R. D. Brown, *Aust. J. Phys.*, 1974, **27**, 425–430.
50 J. L. Holmes and F. P. Lossing, *J. Am. Chem. Soc.*, 1982, **104**, 2648–2649.
51 R. Taylor, *Int. J. Chem. Kinet.*, 1987, **19**, 709–713.